PHYSICAL REVIEW B **68**, 073303 (2003)

Role of electron tunneling in spin filtering at ferromagnet/semiconductor interfaces

S. E. Andresen
Niels Bohr Institute fAPG, Ørsted Laboratory, University of Copenhagen, Universitetsparken 5, 2100 København Ø, Denmark

S. J. Steinmuller, A. Ionescu, G. Wastlbauer, C. M. Guertler, and J. A. C. Bland*
Cavendish Laboratory, University of Cambridge, Madingley Road, Cambridge CB3 0HE, United Kingdom
(Received 3 June 2003; published 25 August 2003)

Spin-dependent electron transport between a semiconductor and a ferromagnetic metal has been studied by polarized photoexcitation. Using a band gap engineered Au/NiFe/GaAs/AlGaAs/n-GaAs structure we are able to precisely control the bias and temperature range under which tunneling processes occur. We find that electron spin filtering is only observed when tunneling processes are switched on, whereas when tunneling is suppressed, only magneto-optical dichroism effects contribute to the polarization dependent photocurrent.

DOI: 10.1103/PhysRevB.68.073303 PACS number(s): 72.25.−b, 73.40.−c, 78.66.−w

Recently the newly emerging field of spintronics has attracted vast interest.[1,2] Spin analog to conventional electronic devices, exploiting the spin rather than the charge of the electrons, could offer significant advances in device performance.[3,4] However, the prerequisite for the realization of such devices is a better understanding of spin-dependent electron transport, including both spin injection from a ferromagnet (FM) into a semiconductor (SC) and spin detection of electrons passing from the SC to the FM. Successful spin injection from a FM metal into SC quantum well structures has been demonstrated recently by several groups.[5–7] It has been pointed out by Schmidt *et al.*[8] that efficient spin transmission across the FM/SC interface will be difficult to achieve in the diffusive transport regime, due to the large conductivity mismatch between a metal and a SC. This problem can be overcome, however, by introducing a tunnel barrier at the FM/SC interface.[9] In this case a large spin dependence can be expected for tunneling electrons.

Our group has recently demonstrated efficient spin detection at room temperature in FM/GaAs Schottky barrier structures using photoexcitation techniques.[10,11] In order to excite spin polarized electrons in the GaAs we use circularly polarized light that is shone on the top surface of the sample and passes the FM layer before reaching the GaAs. This gives rise to magneto-optical dichroism that contributes to the measured helicity dependent photocurrent (HDPC). We conclude from the observed bias dependence of the HDPC that strongly spin dependent transport of electrons passing from the SC to the FM occurs independently of any magneto-optical effects. However, it is an open question, which of the possible charge transport mechanisms between the SC and the FM (hole diffusion into the FM, thermionic emission of electrons over the Schottky barrier, electron tunneling across the Schottky barrier) are spin dependent and therefore will contribute to the signal we observe. In the present study we report on measurements of band gap engineered FM/AlGaAs tunnel barrier/SC structures that enable us to precisely determine the bias and temperature conditions for the different transport regimes. We are therefore able to separate magneto-optical effects and to specify the transport mechanism crucial for spin filtering of electrons passing from the SC to the FM. We find that a significant spin dependence in this spin filtering process can only be expected for tunneling electrons.

The structure is grown by combined SC and metal molecular beam epitaxy in two distinct growth chambers. The SC part of the structure is grown on a n-GaAs(100) substrate under a background pressure in the low 10^{-10} mbar range at 580 °C after oxide desorption at 620 °C in As_2 flux. The layer sequence consists of a 200 nm Si doped (10^{16} cm^{-3}) GaAs buffer, a 2 nm non-doped AlGaAs barrier, and a 2 nm Si doped (10^{18} cm^{-3}) GaAs spacer. An amorphous As cap is deposited for protection against surface oxidation during transfer, and PdGe is deposited for the backside contact. The metal growth takes place at room temperature under a background pressure in the low 10^{-10} mbar range after first desorbing the As cap by annealing at 450 °C for 30 min and checking the surface reconstruction by low-energy electron diffraction. A 5 nm NiFe magnetic layer is deposited followed by a 3 nm Au cap to prevent oxidation. A detailed description of the metal growth system can be found in Ref. 12. Finally Au contacts are grown on top of the capping layer by thermal evaporation.

All measurements were carried out in a constant flow liquid helium cryostat located between the pole pieces of an electromagnet with the magnetic field (maximum 10 kOe) applied along the plane of the FM film. Optical access to the sample was provided by two windows positioned outside the magnet. As a light source we used a diode laser with a wavelength of 785 nm, corresponding to a photon energy of 1.58 eV. The light was shone on the sample at an angle of 22.5° with respect to the plane normal. A photoelastic modulator (PEM) operated at 50 kHz was used to alter the circular polarization of the light and the HDPC [which is proportional to the difference in photocurrent (PC) for illumination with right and left circularly polarized light, respectively[10]] was measured using a lock-in amplifier. The PC was determined by modulating the intensity of the light beam at 100 kHz in a separate measurement using the PEM and an additional linear polarizer. All electrical measurements, i.e., current-voltage characteristics, PC and HDPC measurements, were carried out in a three-contact geometry: The current was measured between one top contact and the bot-

 ©2003 The American Physical Society

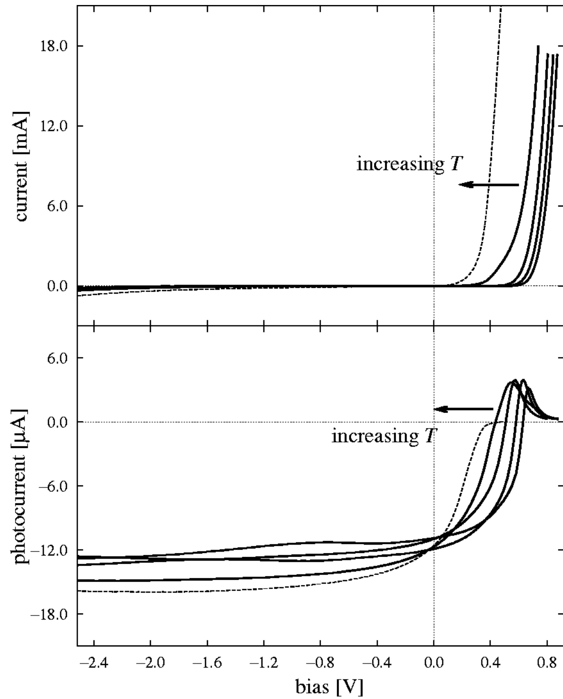

FIG. 1. Bias dependence of the current without photoexcitation (top) and the photocurrent induced by photoexcitation (bottom) at different temperatures of 80, 160, 240, 320, and 360 K.

tom contact and the voltage drop across the sample was measured between the other top contact and the bottom contact.[10,11]

Basic characterization of the structure was carried out by measuring the current-voltage and PC-voltage characteristics using standard methods. Representative results are shown in Fig. 1. The current-voltage characteristic shows an extremely suppressed current level at reverse bias, while an exponentially increasing current level is observed at forward bias exceeding a certain onset voltage in the range 0.4–0.6 V. The PC-voltage characteristic shows a rather stable negative PC level at reverse bias, while a positive PC peak is observed at forward bias exceeding the onset voltage of 0.4–0.6 V. A transition is evident at a temperature of about 300 K, observed as an abrupt decrease in onset voltage and a total suppression of the PC peak.

In order to fully understand the characteristics, we consider a simple model of the band bending at different bias conditions as sketched in Fig. 2. Pinning of the Fermi level in the FM metal within the band gap of the SC gives rise to depletion and accumulation of carriers.[13] Thus the band bending takes place according to the Poisson equation

$$-\nabla^2\varphi = e(n_{\mathrm{dope}} - n_{\mathrm{e}} + n_{\mathrm{h}}), \tag{1}$$

with φ the electric potential, e the electron charge, n_{dope} the doping density, and n_e and n_h the electron and hole densities, respectively. At the zero bias condition electron depletion occurs with the resulting band bending as illustrated in Fig. 2(c). This implies a negative PC originating from electrons diffusing into the SC and holes tunneling into the FM metal. As illustrated in Fig. 2(b) a certain value of the forward bias

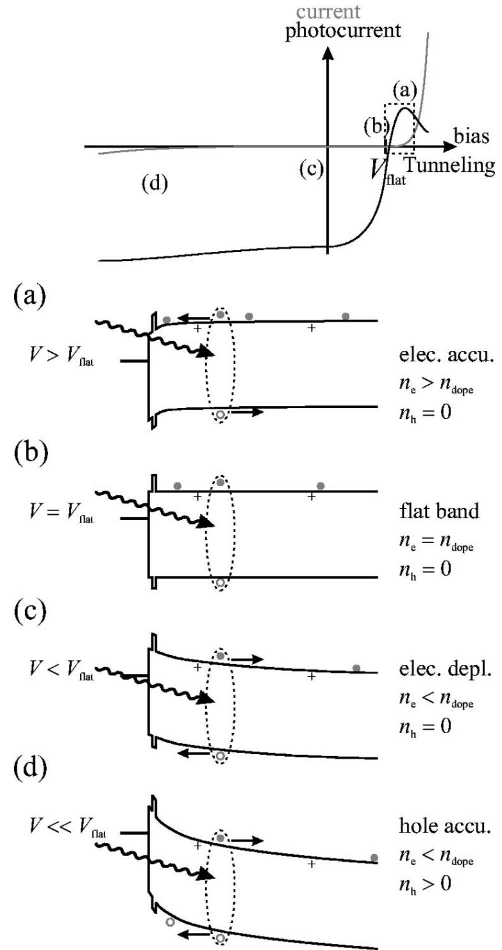

FIG. 2. Schematics of the band bending and the corresponding current-voltage and photocurrent-voltage characteristics in the case of (a) forward bias electron accumulation, (b) forward bias flat band configuration, (c) zero bias electron depletion, and (d) reverse bias hole accumulation.

voltage V_{flat} will give rise to a flat band configuration with neither electron depletion nor accumulation. The vanishing internal electric field gives rise to a vanishing PC. Figure 2(a) shows that electron accumulation near the barrier takes over at forward bias exceeding V_{flat}. Electrons tunneling into the FM metal and holes diffusing into the SC give rise to a positive PC at forward bias moderately exceeding V_{flat}. As the forward bias is further increased, the electron accumulation region is narrowed, and the PC decreases rapidly. In contrast, hole accumulation occurs over an extensive reverse bias range as illustrated in Fig. 2(d), causing less pronounced variations in PC as the bias is changed.

A comparison of the results of the characterization measurements shown in Fig. 1 with the model in Fig. 2 allows an identification of the bias regime in which electron tunneling occurs for both current and PC. This is the case for forward bias values moderately exceeding V_{flat} as sketched in Fig. 2(a), which coincide with the PC peak in Fig. 1 at about 0.4–0.8 V. The strong reduction in onset voltage at about 300 K reveals that thermal emission over the AlGaAs barrier becomes significant at this temperature, leaving the Schottky

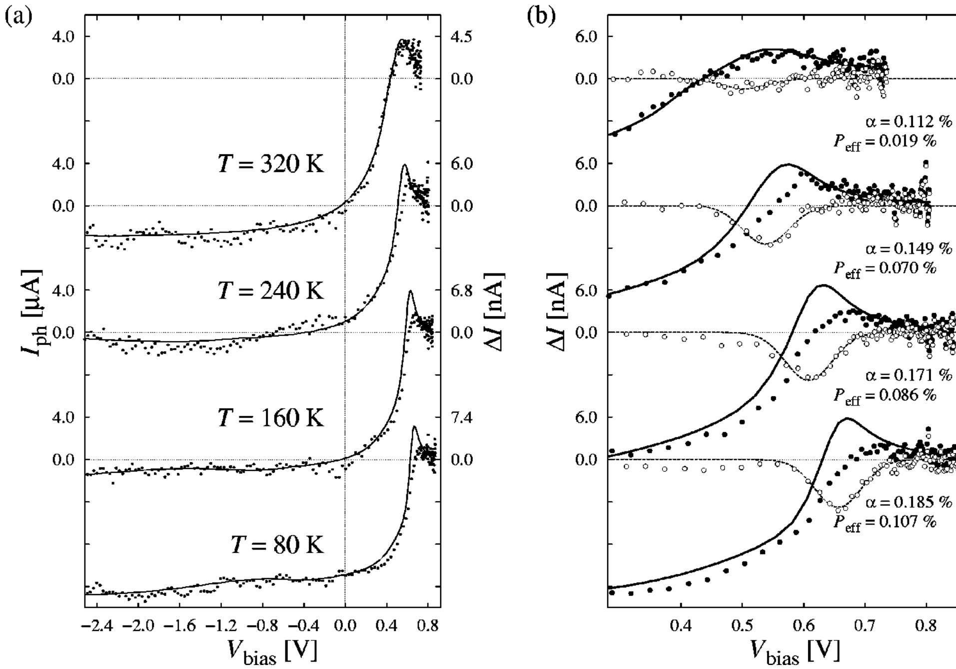

FIG. 3. (a) Comparative plots of the photocurrent I_{ph} (solid lines) and the magnitude of the helicity-dependent photocurrent ΔI (points) versus bias voltage V_{bias} at different temperatures. (b) Separation of the total helicity-dependent photocurrent ΔI (solid circles) into the magneto-optical contribution $\Delta I_{MCD} = \alpha I_{ph}$ (solid lines) and the contribution due to spin filtering $\Delta I_{SF} = \Delta I - \alpha I_{ph}$ (open circles) with parameters α and P_{eff} given by Eq. (4). The dashed line is a guide to the eye, and the sequence of temperatures is the same as that shown in (a).

barrier to determine the electron transport process. Thus tunneling is suppressed at elevated temperatures, which causes the peak in the PC to vanish. In this way the PC peak is attributed to electron tunneling through the AlGaAs barrier, suppressed by thermal emission as temperature is increased.

The excess energy of the excited carriers has not been taken into account, since the transport processes are governed by the bend bending. The excess energy is given by the difference between the excitation energy of 1.58 eV and the band gap energy, which varies with temperature in the range 1.52–1.42 eV.[14] The resulting excess energies of 0.06–0.16 eV are under all circumstances insufficient for overcoming the barrier height of about 0.49–0.44 eV.

The dependence of the HDPC on magnetic field follows the hysteresis loop of the magnetic film with a constant offset as observed in previous studies.[10,11] The offset is only present at nonperpendicular angles of light incidence, and its independence of the magnetic field strength proves that it arises purely due to optical effects. In order to remove the contribution from the nonmagnetic offset to the HDPC, a magnetic field of 260 Oe is applied (sufficient to saturate the magnetic film), and the HDPC for opposite field directions are subtracted. Thus the magnitude (ΔI) of the HDPC is given by the relation (using a slightly different notation here to that followed by Hirohata *et al.*[10,11])

$$\Delta I = \frac{I^+ - I^-}{2}, \tag{2}$$

with the HDPC I^+ and I^- for positive and negative saturation, respectively.

Figure 3(a) shows measurements of the bias dependence of both the PC and the magnitude of the HDPC at different temperatures. The bias dependence of the two currents at reverse bias is exactly the same for all temperatures, as is evident from scaling the HDPC to the PC [Fig. 3(a)]. On the contrary a pronounced discrepancy is observed at forward bias, coinciding with the PC peak at 0.4–0.8 V, which was identified above as the bias regime in which electron tunneling occurs.

Different transport mechanisms (hole diffusion into the FM, thermionic emission of electrons over the AlGaAs barrier, electron tunneling across the AlGaAs barrier) will contribute to the nonpolarized PC, according to the applied bias. In principle all of these processes could be spin dependent and therefore contribute to the HDPC. Significant spin filtering effects would be expected to occur at reverse bias in the case of spin dependent hole transport, and at forward bias in the case of spin-dependent electron transport, respectively. As in our geometry the light has to pass the FM layer before entering the GaAs, there will also be a contribution of magnetic circular dichroism (MCD) to the HDPC. Therefore ΔI will, in general, be a superposition of magneto-optical (ΔI_{MCD}) as well as spin filtering (ΔI_{SF}) effects:

$$\Delta I = \Delta I_{SF} + \Delta I_{MCD}, \tag{3}$$

with ΔI_{MCD} being proportional to the nonpolarized PC ($\Delta I_{MCD} = \alpha I_{ph}$).

The well-defined structure of our sample allows a clear separation of all these contributions. As pointed out previously, a significant difference between the bias dependences of the nonpolarized PC and the HDPC was only observed at forward bias (0.4–0.8 V), where electron tunneling occurs, whereas the bias dependences of both currents match each other closely at reverse bias. The latter finding clearly shows that spin-dependent hole transport does not play an important role and that the HDPC at reverse bias arises mainly from MCD. We are therefore able to fit the parameter α by comparing the bias dependences of the PC and the HDPC at reverse bias and to subtract the contribution of ΔI_{MCD} from

the total HDPC [Fig. 3(b)]. The spin filtering efficiency can then be quantified in terms of an effective polarization P_{eff}, defined as

$$P_{\text{eff}}=\frac{\Delta I-\alpha I_{\text{ph}}}{2I_{\text{ph}}}. \tag{4}$$

P_{eff} is an indirect measure of the polarization of the tunneling electrons since the true tunneling current cannot be separated from I_{ph} and is likely to be much smaller than the total PC. It can, however, be used to determine the relative change in electron polarization with temperature. We found that P_{eff} is of the order 0.1% and decreases with increasing temperature. At about 300 K, where thermionic emission significantly contributes to the transport process, as pointed out above, P_{eff} approaches zero. As shown in Fig. 3(b), practically no spin filtering was observed at this temperature. Hence any spin dependent contribution of electrons thermionically emitted over the barrier can be ruled out. This finding can be explained in a very simplified view by the fact, that once, the electrons have overcome the barrier, a large number of states will be available in the metal for either spin orientation.

Our combined data unambiguously proves that only tunneling electrons show a significant spin dependence. This finding is in good agreement with the spin filtering mechanism proposed in earlier papers,[10,11] but goes much further in separating magnetic circular dichroism effects and explicitly ruling out any spin-dependent contributions from hole transport or thermionic emission. In our model, electrons tunneling through the barrier will, dependent on their spin orientation, have a different number of states available to tunnel into, due to the spin-split density of states in the FM. This mechanism is highly spin sensitive, similar to the tunneling process in magnetic tunnel junctions,[15,16] where, instead of an optically pumped SC, a FM metal is used as a spin injector. There are, however, fundamental differences between these two approaches, due to the different electrical properties and band structures of SC and FM metals.

In conclusion we have investigated spin dependent electron transport across the FM/SC interface by introducing a band gap engineered tunneling barrier. Efficient spin filtering was only observed at forward bias, where electron tunneling occurs. On the other hand, at reverse bias where tunneling is suppressed, this process is switched off and only magnetic dichroism effects contribute to the helicity dependent photocurrent. In this way we were able to distinguish between spin filtering and magneto-optical dichroism allowing us to quantify the contribution of each mechanism to the helicity dependent photocurrent. The effective polarization of the tunneling electrons was found to decrease with increasing temperature, approaching zero when thermal emission becomes dominant at about 300 K. From these combined results we are able to unambiguously show that spin filtering is associated with electron tunneling and that the thermionic emission process is spin independent.

S.E.A. acknowledges the financial support from the Danish Technical Research Council materials framework program. S.J.S. would like to thank EPSRC and ABB Sweden for their funding. G.W. is grateful for the financial support of the Austrian Academy of Sciences, the Wilhelm-Macke-Stipendienprivatstiftung (Austria), and the Cambridge Philosophical Society (UK). A.I. thanks the Cambridge European Trust and Nordiko Ltd. for their funding.

*Electronic address: jacb1@phy.cam.ac.uk

[1] G. Prinz, Science **282**, 1660 (1998).
[2] P. Ball, Nature (London) **404**, 918 (2000).
[3] S. Datta and B. Das, Appl. Phys. Lett. **56**, 665 (1990).
[4] R. Fiederling, M. Keim, G. Reuscher, W. Ossau, G. Schmidt, A. Waag, and L.W. Molenkamp, Nature (London) **402**, 787 (1999).
[5] H.J. Zhu, M. Ramsteiner, H. Kostial, M. Wassermeier, H.-P. Schönherr, and K.H. Ploog, Phys. Rev. Lett. **87**, 016601 (2001).
[6] A.T. Hanbicki, B.T. Jonker, G. Itskos, G. Kioseoglou, and A. Petrou, Appl. Phys. Lett. **80**, 1240 (2002).
[7] V.F. Motsnyi, J. De Boeck, J. Das, W. Van Roy, G. Borghs, E. Goovaerts, and V.I. Safarov, Appl. Phys. Lett. **81**, 265 (2002).
[8] G. Schmidt, D. Ferrand, L.W. Molenkamp, A.T. Filip, and B.J. van Wees, Phys. Rev. B **62**, R4790 (2000).
[9] E.I. Rashba, Phys. Rev. B **62**, R16 267 (2000).
[10] A. Hirohata, Y.B. Xu, C.M. Guertler, J.A.C. Bland, and S.N. Holmes, Phys. Rev. B **63**, 104425 (2001).
[11] A. Hirohata, S.J. Steinmueller, W.S. Cho, Y.B. Xu, C.M. Guertler, G. Wastlbauer, J.A.C. Bland, and S.N. Holmes, Phys. Rev. B **66**, 035330 (2002).
[12] Y.B. Xu, E.T.M. Kernohan, D.J. Freeland, A. Ercole, M. Tselepi, and J.A.C. Bland, Phys. Rev. B **58**, 890 (1998).
[13] S.M. Sze, *Semiconductor Devices* (Wiley, New York, 1985).
[14] J.S. Blakemore, J. Appl. Phys. **53**, 502 (1982).
[15] M. Julliere, Phys. Lett. **54A**, 225 (1975).
[16] J.S. Moodera, L.R. Kinder, T.M. Wong, and R. Meservey, Phys. Rev. Lett. **74**, 3273 (1995); T. Miyazaki, T. Yaoi, and S. Ishio, J. Magn. Magn. Mater. **98**, L7 (1991).